Pharm Res (2014) 31:1724–1734
DOI 10.1007/s11095-013-1275-1

RESEARCH PAPER

# Direct Microneedle Array Fabrication Off a Photomask to Deliver Collagen Through Skin

Jaspreet Singh Kochhar • Parthiban Anbalagan • Sandeep Balu Shelar • Jun Kai Neo • Ciprian Iliescu • Lifeng Kang

Received: 1 October 2013 / Accepted: 19 December 2013 / Published online: 22 January 2014


## ABSTRACT

***Purpose*** To fabricate microneedle arrays directly off a photomask using a simple photolithographical approach and evaluate their potential for delivering collagen.

***Methods*** A simple photolithographical approach was developed by using photomask consisting of embedded micro-lenses that govern microneedle geometry in a mould free process. Microneedle length was controlled by use of simple glass scaffolds as well as addition of backing layer. The fabricated arrays were tested for their mechanical properties by using a force gauge as well as insertion into human skin with trypan blue staining. Microneedle arrays were then evaluated for the delivery of fluorescent collagen, which was evaluated using a confocal laser scanning microscope.

***Results*** Microneedles with sharp tips ranging between 41.5 ± 8.4 $\mu$m and 71.6 ± 13.7 $\mu$m as well as of two different lengths of 1336 ± 193 $\mu$m and 957 ± 171 $\mu$m were fabricated by using the photomasks. The microneedles were robust and resisted fracture forces up to 25 N. They were also shown to penetrate cadaver human skin samples with ease; especially microneedle arrays with shorter length of 957 $\mu$m penetrated up to 72% of needles. The needles were shown to enhance permeation of collagen through cadaver rat skin, as compared to passive diffusion of collagen.

***Conclusions*** A simple and mould free approach of fabricating polymeric microneedle array is proposed. The fabricated microneedle arrays enhance collagen permeation through skin.

**KEY WORDS** collagen · microneedles · photolithography · transdermal drug delivery

## INTRODUCTION

Biopharmaceuticals are increasingly gaining prominence in the pharmaceutical and cosmetic industry. However, unlike conventional drugs that can be administered via non-invasive routes, biopharmaceuticals such as proteins usually require hypodermic injection, causing inconvenience and reduced compliance among patients especially in children and the elderly.

Transdermal drug delivery has been proposed as an alternative route for the administration of drugs to overcome the limitations posed by hypodermic injection. Several commercial products, such as nicotine transdermal patch, that allows effective drug delivery via transdermal administration have been developed. However, the number of drug molecules that qualify for transdermal delivery is limited due to the presence of lipophilic stratum corneum, the outermost layer of skin, acting as a physical barrier.

To overcome this limitation, micron-scale needles can be utilized to create pores through the stratum corneum, thus allowing the passage of big molecules. Peptides such as insulin, desmopressin, human growth hormone and vaccines have been demonstrated to achieve adequate physiological activity after passage through microneedle treated skin (1–3). In a recent clinical study, microneedles were used for transcutaneous immunization and were shown to increase antibody titer levels without having any adverse effect on 20 healthy volunteers (4).

Recent advancements have enabled polymers and sugars to be used to fabricate microneedles (5,6). Various fabrication methods have been used to form polymeric microneedles. One of the common methods employed by researchers is micromolding in which molds of the desired microneedle

**Electronic supplementary material** The online version of this article (doi:10.1007/s11095-013-1275-1) contains supplementary material, which is available to authorized users.

J. S. Kochhar • P. Anbalagan • S. B. Shelar • J. K. Neo • L. Kang (✉)
Department of Pharmacy, National University of Singapore
18 Science Drive 4, Singapore 117543, Singapore
e-mail: lkang@nus.edu.sg

C. Iliescu
Agency for Science, Technology and Research
Institute of Bioengineering and Nanotechnology
31 Biopolis Way, the Nanos, #04-01, Singapore 138669, Singapore

geometry are constructed using high-aspect-ratio SU-8 epoxy photoresist or polyurethane master structures to form PDMS (polydimethylsiloxane) molds from which biodegradable polymer microneedle replicates are formed (7,8). However, this approach involves multiple steps and the use of toxic SU-8 epoxy in the intermediate processes (9).

In a previously developed method in our lab, photolithography using photomasks was used as an alternative to fabricate polymeric microneedles in a single step, mould free process (10). Macromer was exposed to high intensity ultraviolet (UV) light through a patterned film in the presence of a photo initiator to form crosslinked polymeric rods. Free radicals formed by the photoinitiator propagate the polymerization reaction. This method offers the advantage of a short fabrication time and a greater suitability of scaling up commercially for industrial purposes. However, as no mechanism to optically modify the light path was involved, the formed microneedles had a blunt tip.

In this study, we developed a simple photolithographical process using microlenses to fabricate polymeric microneedles of increased sharpness. Although previous studies have involved the use of microlenses to fabricate polymeric microneedles, those methods were limited by involvement of multiple complicated steps (7). Mechanical properties of the microneedles were characterized to ensure their suitability for efficient penetration through excised skin samples (9,10). Finally, evaluation of usability of the resultant microneedles in the transdermal delivery of collagen was performed on rat skin. To our knowledge, this is the first study demonstrating that collagen I molecules could be externally delivered through skin using a microneedle device.

## MATERIALS AND METHODS

### Materials

Poly (ethylene glycol) diacrylate (PEGDA, Mn = 258), 2-hydroxy-2-methyl-propiophenone (HMP), bovine collagen type I, FITC conjugate and trypan blue solution (0.4%) were purchased from Sigma-Aldrich (St. Louis, MO). All materials were reagent grade and were used as received.

### Photomask Fabrication

A 4" Pyrex glass wafer (Corning 7740) was first cleaned in piranha ($H_2SO_4/H_2O_2$) for 20 min at 120°C as shown in Fig. 1a. Later an e-beam evaporator was used to deposit a Chromium/Gold (Cr/Au) layer (30 nm/1 μm) (11) on the glass wafer. A classical photolithographic process using an AZ7220 positive photoresist was utilized to create patterns in the Cr/Au layer using Cr and Au etchants. In order to increase the quality of the Cr/Au/photoresist masking layer, a hard baking process was performed on a hot plate at 120°C for 30 min (12). The opposite surface of the glass wafer was temporary bonded using wax on a dummy silicon wafer in order to conserve the quality of the surface during the wet etching process. Isotropic etching of the lens was performed using an optimized hydrofluoric acid (49%)/hydrochloric acid (37%) in 10/1 volumetric ratio (13) using magnetic stirring for 8.5 min (having an etching rate of 7 μm/min). Separation of glass wafer from the dummy silicon wafer was performed by placing on a hot plate (at 100°C). Over-hanging photoresist and Cr/Au layers at the edges of the lenses were removed by ultrasonication. Finally, removal of the photoresist mask and residual wax was done by cleaning in *N*-Methyl-2-pyrrolidone at 80°C in an ultrasonic tank. Microscopic analysis of the photomask dimensions was performed by directly imaging the photomask and the PDMS mold replicas copied from the microlenses with a scanning electron microscope and Nikon SMZ 1500 stereomicroscope (Nikon, Japan), respectively.

### Fabrication of Microneedle Shafts

A photomask (1 × 1 cm) consisting of an array of 7 × 7 embedded lenses was used for the fabrication process. A cavity, measuring 2.5 × 0.9 cm, was created using glass slides as shown in Fig. 1b. The number of glass slides used determines the height of the cavity (referred to as spacer thickness). Increased spacer thickness was achieved by increasing the number of glass slides stacked on either side of the glass. The photomask was positioned to ensure that the Cr/Au coated surface faced the interior of the cavity with none of the lenses being obscured by the sides of the cavity walls. PEGDA, containing 0.5% w/w HMP (referred to as prepolymer solution) was filled into the cavity until the Cr/Au coated surface was in contact with the solution without any visible bubbles. The setup was then irradiated with high intensity ultraviolet light of the desired intensity for 1 s at the distance of 3.5 cm from the UV source using UV curing station with a UV filter range of 320–500 nm (OmniCure S200-XL, EXFO Photonic Solutions Inc., Canada). The intensity of the UV light was measured with the OmniCure R2000 radiometer. A collimating adaptor (EXFO 810-00042) was used with the UV light probe. After exposure to UV light, the photomask with the array of needles was removed and the remaining prepolymer solution could be reused. The use of the photomask blocked the UV access in the Cr/Au-coated regions and allowed UV light to pass through the embedded lenses followed by subsequent refraction of light rays to a focal point that determines the height of the microneedles formed. The prepared microneedles were then imaged using Nikon SMZ 1500 stereomicroscope (Nikon, Japan), to quantify the microneedle length and tip diameter.

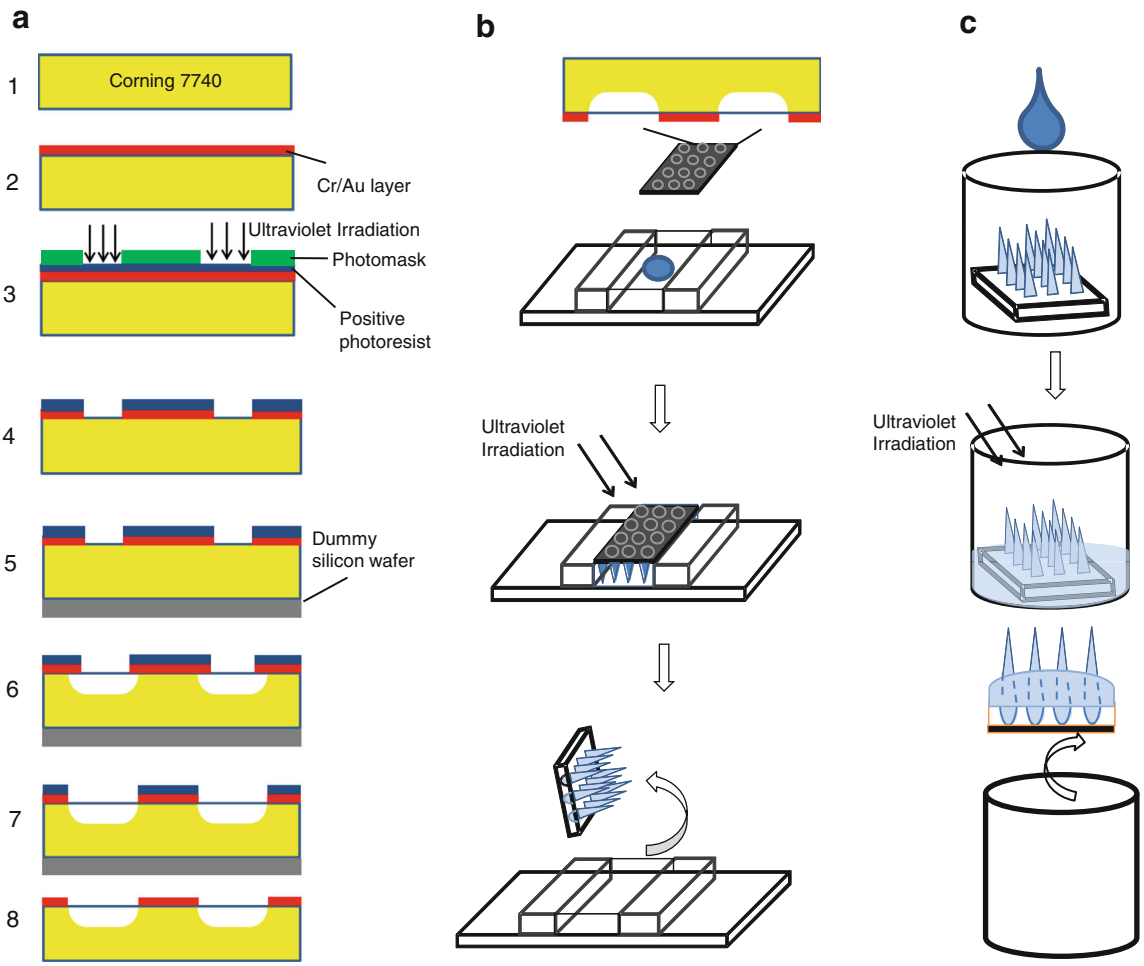


**Fig. 1** (**a**) Schematic representation of the fabrication process of lenses embedded photomask. (*1*) 4" glass wafer. (*2*) Cr/Au layer deposited using an e-beam evaporator. (*3*) Exposure of Cr/Au/photoresist masking layer to UV light with photomask. (*4*) Formation of pattern on layer using Cr and Au etchants. (*5*) Temporary bonding of glass on a dummy silicon wafer. (*6*) – (*7*) Wet etching (isotropic) process using HF/HCl etchants followed by ultrasonication. (*8*) Debonding of dummy silicon wafer and removal of photoresist layer. (**b**) Schematic representation of the fabrication process of needles. Cr/Au coated photomask (7 × 7 array), is placed over a cavity containing pre-polymer solution and exposed to UV irradiation. (**c**) Schematic representation of the fabrication process of the backing layer. Photomask, with microneedles attached, is placed in a well filled with pre-polymer and exposed to UV irradiation.

## Microneedle Backing Layer Fabrication

The photomask with needles was placed in a well of a 24-well plate (Thermo Fisher Scientific, USA) as shown in Fig. 1c. A specified volume (300 and 400 μL) of prepolymer solution was added to the well until the needles were submerged to a desired height. The volume of prepolymer solution used determines the thickness of the backing layer. The set up was then irradiated with high intensity ultraviolet light (15.1 W/cm$^2$) from a distance of 10.5 cm from the UV source for a duration of 1 s. After polymerization, the microneedle with the backing layer was separated from the photomask. Microneedles of two different lengths with minimal differences in tip diameter could be achieved via this method. The prepared microneedles with the backing layer were then imaged using Leica M205FA stereomicroscope (Leica Microsystems, Germany), to quantify the microneedle length, tip diameter and base diameter.

## Microneedle Fracture Force Testing

Microneedles of two different lengths were pressed against an aluminium plate with a force applied by a Dillon GL-500 digital force gauge (Dillon, USA) (14). The applied force was increased until maximum resistance was observed. The force at which microneedles start to break (fracture force) was recorded after which microneedles were imaged using Nikon AZ100 stereomicroscope (Nikon, Japan), to assess the changes in the microneedle geometric characteristics.

## Microneedle Penetration in Cadaver Human Skin

Microneedles of two different average lengths were inserted into cadaver human back skin obtained through posthumous organ donation by a 75 year old, white female. The use of human skin for this study was approved by the National

University of Singapore Institutional Review Board (No. 13-167E). The skin was laid stretched on a board and microneedle shafts of both lengths were inserted using the force of a thumb for 1 min. The microneedles were then removed and the area of insertion was stained with trypan blue for 12 min. Trypan blue, being hydrophobic in nature, specifically stains the hydrophobic perforated stratum corneum sites. Intact skin stained with trypan blue was used as a negative control. The excess stain was wiped away using Kimwipes® and ethanol (70%). The areas stained with the dye were viewed by brightfield microscopy using Eikona Image Soft Microscope (China).

### Collagen Permeation Through Rat Skin

Microneedles of the shorter microneedle length were inserted into excised rat abdominal skin. The hair was first removed using hair removal cream Veet® (Reckitt Benckiser, Poland) (15). The skin samples were cleaned and the subcutaneous fat was removed using a scalpel. The skin was fully stretched on ten layers of Kimwipes® (Kimberly-Clark, Roswell, GA) to mimic tissue-like mechanical support (16). A force of 10 Newton (N) (17) was applied using the Dillon GL-500 digital force gauge (14) for 2 min. Bovine skin collagen type I, FITC conjugate (Mn = 300 kDa) of concentrations 0.025, 0.050 and 0.075% w/v was obtained by diluting the stock collagen solution (0.1% w/v) with appropriate amount of 0.1 M Tris–HCl buffer (pH 7.8) containing 0.4 M NaCl, 10 mM $CaCl_2$ and 0.25 M glucose (18). NaCl and $CaCl_2$ aid in stabilizing the collagen molecules and glucose is added to prevent gelation of the collagen fibers (18). Each collagen concentration was applied to separate skin samples at the area of insertion. The time of contact between the collagen solution and the skin was kept constant at 4 h (1) at room temperature, after which excess collagen on the skin surface was removed using Kimwipes®. The degree of permeation of collagen through the skin was quantified by using the A-1R confocal microscope (Nikon, Japan) to observe the fluorescence intensity of collagen type I, FITC conjugate at excitation and emission wavelengths of 490 nm and 520 nm respectively. Other parameters including high voltage (150), offset (-1), laser (7.2% of 150 mW), pinhole (1.2 A.U), optical sectioning (16.6 μm), scan size (512×512), scan speed (1 frame/sec), pixel dwell (2.2 μsec), lever average (4), zoom (5×), step size (5 μm) and intensity calculation (low = 300, high = 4,095) were kept constant. All animal experiments were approved by Institutional Animal Care and Use Committee, National University of Singapore.

### Statistical Analysis

Testing of microneedle geometric properties involved three microneedle arrays being fabricated for each parameter studied and mean ± standard deviation was reported. Statistical analysis of the data was performed using PASW Statistics 18 Software (SPSS Inc, Chicago, IL). One-way ANOVA was used, for analyzing multiple groups of data or statistical differences. Results with $p$ value of less than 0.05 were considered to be statistically significant.

## RESULTS

### Fabrication of Photomask

The characteristics of the photomask and the embedded microlenses affect the geometry of the microneedles significantly as the path of the UV rays are dependent on the degree of refraction on the convex surface of microlenses (Fig. 2a). All photomasks consisted of an array of microlenses (7×7) with a constant center-to-center spacing of 1,000 μm. Analysis of microlenses revealed that each microlens has a diameter of 350 μm with a flattened convex surface of diameter 130 μm, and a depth of 62.3 μm as shown in Fig. 2b–d. To evaluate the estimated focal length (f) of the microlens, radius of curvature of the first surface was calculated to be 272.89 μm by using Pythagoras theorem. Considering these parameters and the refractive index of both glass (1.53627) and air (1.000) at a wavelength of 365 nm, the focal length was estimated to be 509.28 μm via the Lens maker's equation as stated below:

$$1/f = (n_1/n_m - 1) * (1/r_1 - 1/r_2)$$

where $n_1$ is the refractive index of lens material, $n_m$ is the refractive index of ambient medium, $r_1$ is the radius of curvature of the first surface, $r_2$ is the radius of curvature of the second surface.

### Fabrication of Polymeric Microneedles

#### *Effect of Intensity of UV Light*

The intensity of UV light was varied between 3.14 and 15.1 W/cm$^2$ maintaining the spacer thickness (5 mm), and distance from UV light source (3.5 cm) constant. Average microneedle length was found to increase from 2,358 ± 144 μm to 4,035 ± 293 μm when intensity was increased from 3.14 to 9.58 W/cm$^2$ ($p < 0.05$) (Fig. 3a). However, the difference in average length measured for the needles formed for the intensities 9.58 to 15.1 W/cm$^2$ was found to be insignificant ($p > 0.05$). The minimum length obtained is more than three times the estimated microneedle length quantified by the theoretical focal length.

Sharpness, quantified by tip diameter of microneedles, reduced as intensity was increased. Average tip diameter increased from 41.5 ± 8.4 μm to 49.0 ± 5.8 μm for the intensities of 3.14 to 6.44 W/cm$^2$ ($p < 0.05$) as shown is Fig. 3b.

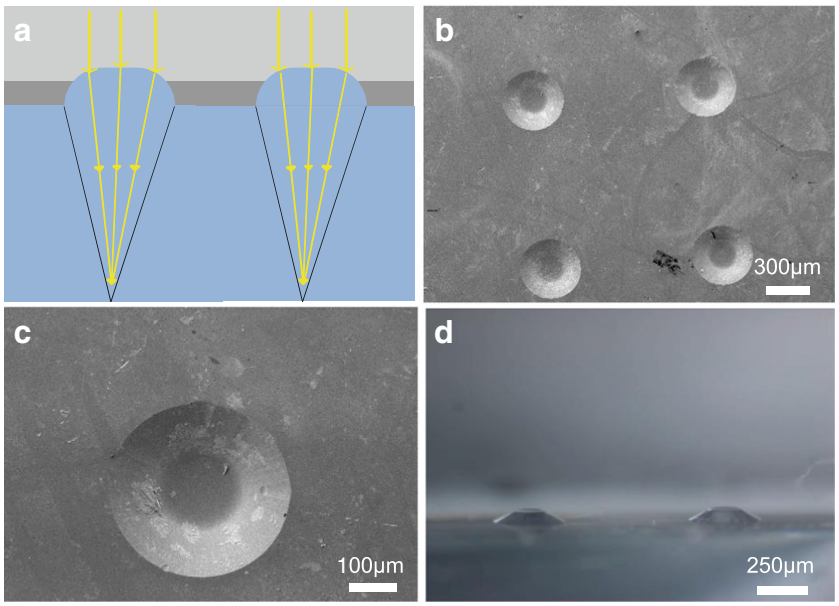


**Fig. 2** Characterization of photomask. (**a**) UV (365 nm) exposure focuses light into a conical path, producing tapered microneedles. (**b** and **c**) A SEM image of a microlens. (**d**) A portion of an array of PDMS mold replicas copied from the microlenses, showing the flattened convex surface, under a stereomicroscope.

However, no significant change in the tip diameter was observed from 6.44 to 12.4 W/cm$^2$, with a maximum tip diameter of 71.6±13.7 μm obtained when an intensity of 15.1 W/cm$^2$ was used. Interestingly, greater level of deformation on the needles was observed as higher intensities were used. It was noted that the microneedles' upper half became wider and more cylindrical with the lower half acquiring a more tapered formation as intensities increased. In addition, the tips of the microneedles also underwent deformations leading to more irregular structures. The microneedles fabricated at 6.44 W/cm$^2$ were observed to be more regular in shape, than that of higher intensities, without significant structural deformation

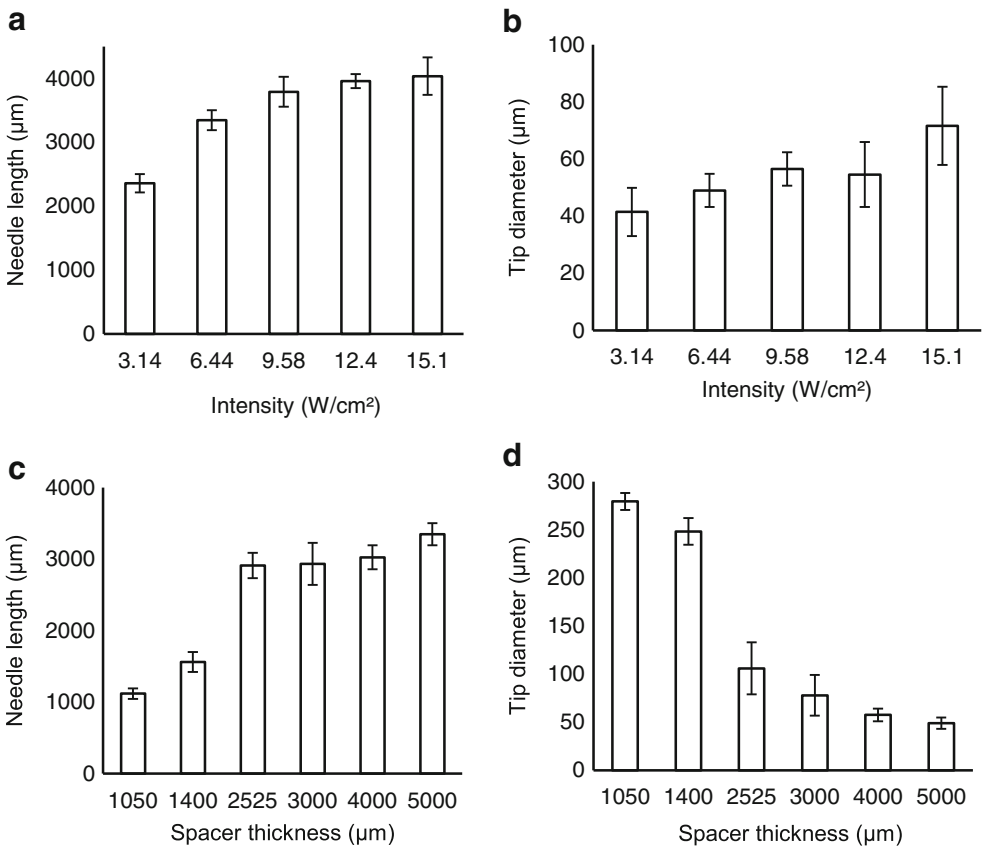


**Fig. 3** Effect of UV parameters on microneedle geometry. Effect of (**a**) intensity and (**c**) spacer thickness on microneedle length. Effect of (**b**) intensity and (**d**) spacer thickness on microneedle tip diameter.

thus preserving the sharpness. Hence, this intensity was chosen for fabrication of microneedles for subsequent experiments.

### *Effect of Spacer Thickness*

The spacer thickness was varied between 1,050 and 5,000 μm maintaining the intensity (6.44 W/cm$^2$), and distance from UV light source (3.5 cm) constant. An expected increase in average length was observed for the spacer thickness of 1,050 to 2,525 μm ($p<0.05$). Insignificant difference in average length was recorded for the needles formed for the spacer thickness of 2,525 μm to 5,000 μm ($p>0.05$). The longest microneedle length of 3,347±156 μm was observed for the needles formed using a spacer thickness of 5,000 μm ($p<0.05$) (Fig. 3c). Average tip diameter decreased as the spacer thickness was increased from 1,050 μm to 3,000 μm ($p<0.05$), with a constant tip diameter reached beyond the spacer thickness of 3,000 μm ($p>0.05$) (Fig. 3d).

## Effect of Backing Layer Volume

Formation of a backing layer is crucial to enhance the strength of the microneedle shafts and to enable the removal of the microneedles from the photomasks, making them reusable. We manipulated the thickness of the backing layer by varying the volume of prepolymer solution. We used two volumes (300 μL and 400 μL). Due to the affinity between the polymerized microneedles and the prepolymer solution together with the small center-to-center spacing between microneedles, capillary action was evident. Subsequent exposure to UV light led to formation of each patch of microneedle acquiring a range of length, with the tip diameter being unaffected as shown in Fig. 4a and b. It was observed that the average microneedle length decreased from 1,336± 193 μm to 957±171 μm as volume used to form the backing layer, was increased from 300 μL to 400 μL (Fig. 4e). Similarly, base diameter reduced from 233±20 μm to 156± 21 μm ($p<0.05$).

## Microneedle Fracture Force Testing

Evaluation of the effect of the thickness of the patch on the strength of microneedles is essential for the selection of the appropriate type of patch for maximum penetration through the skin. After subjecting each class of microneedle array to an increasing force against a flat surface, it was observed that the fracture force was consistent for both classes of patches ($p<0.05$) with a similar negligible degree of breakage for both microneedle arrays below the fracture force as depicted in Fig. 4c, d and f.

## Microneedle Penetration in Human Skin

Microneedles of average length 957 (short) and 1,336 (long) μm were inserted in cadaver human skin. Trypan blue staining method was used to demonstrate the extent of penetration by each type of microneedle shaft as shown in Fig. 5a and b. Negligible staining on the control skin (figure not shown) proved that trypan blue only stains the sites of stratum corneum perforation significantly.

The extent of penetration by the shorter microneedle shafts was found to be higher (72.7±5.1%) as compared to longer shafts (52.3±3.1%), ($p<0.05$) (Fig. 5c and d). This could be attributed to slightly higher fracture force observed in the case of shorter microneedles (Fig. 4f). Fracture of microneedle was not observed in any of the microneedle shafts tested.

## *In Vitro* Collagen Permeation Through Rat Skin

The ability of microneedles to increase skin permeation of bovine collagen type I, FITC conjugate (Mn=300 kDa) was assessed. The control skin (without collagen treatment) was found to possess a significant level of auto fluorescence which was visible up to a depth of 150 μm (Fig. 6a), while application of collagen solution on intact skin did not lead to any significant absorption (Fig. 6b). This phenomenon could be due to the presence of fluorescent biomolecules such as lipofuscin and riboflavin (19–21) on the rat skin which are able to emit light at similar wavelengths used in the experiment. However, this did not hinder the analysis of the increased degree of collagen permeation by the microneedles. With the shorter microneedle of 957 μm applied on skin followed by application of collagen solution of three different concentrations, revealed a penetration to a depth of 250 to 300 μm confirming the increased extent of diffusion of collagen molecules through epidermis as shown in Fig. 6c–e.

# DISCUSSION

Many groups have successfully developed polymeric microneedles using photolithographical methods. Previous studies to develop sharp polymeric microneedles have used multi-step methods involving development of SU–8 master structures to create PDMS molds and the use of lasers (7,22). Development of a simple photolithographical process by us previously involved the use of a planar patterned photomask showed a simple alternative to mould based methods. However, with the use of planar photomasks, UV light passed through straight with little deviation resulting in microneedles with a more cylindrical and less sharp tips.

In this study, we developed a one-step lithographical method utilizing a photomask with integrated convex lenses. Ultraviolet rays undergo refraction at the surface of the lens,

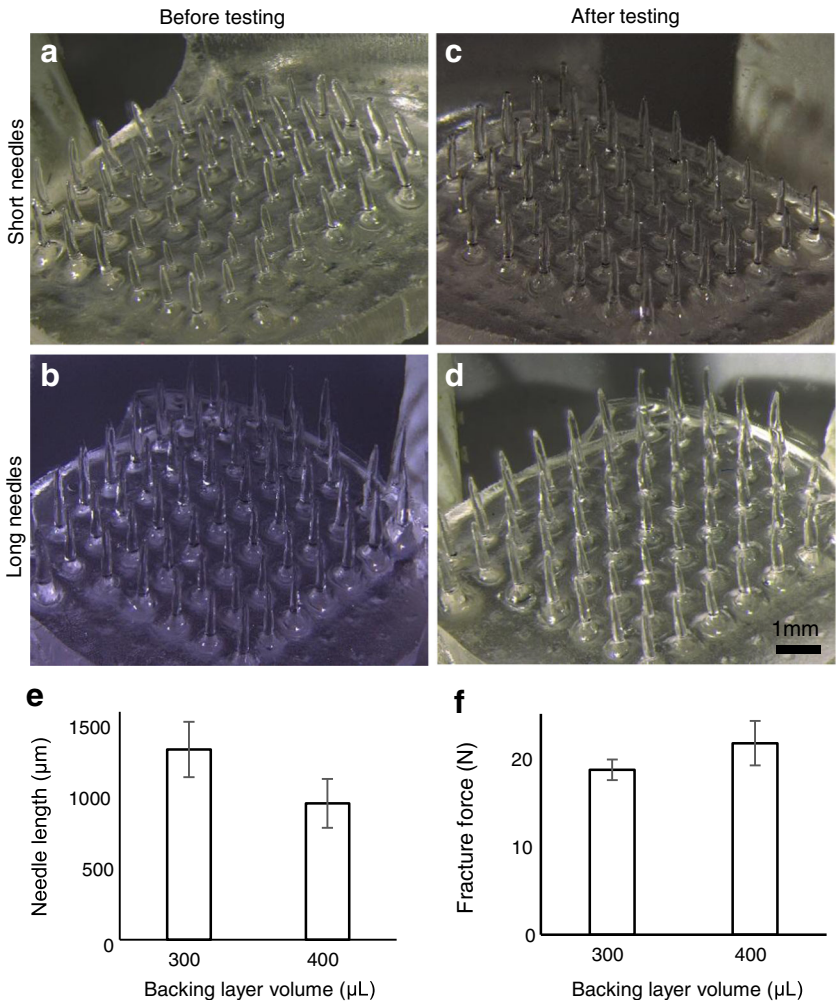


**Fig. 4** Effect of varying pre-polymer volume used for backing layer fabrication. (**a**–**b**) Images at various pre-polymer volume, with average microneedle length for short (957 $\mu$m) and long (1,336 $\mu$m) microneedles respectively. (**c**–**d**) Images corresponding to (**a**–**b**) after fracture force testing. (**e**) Decrease in microneedle length with increase in pre-polymer volume used for backing layer fabrication. (**f**) Microneedle fracture force across the two pre-polymer volumes used to fabricate backing layer.

allowing the rays to converge at a focal point. Polymerization reaction in the presence of UV only occurs in the converged path. This results in sharp-tipped microneedles with improved skin penetration capability than previously fabricated microneedles. While thermal and annealing processes were recently reported for fabrication of microneedles on a curved surface (23), the current approach is amenable for production of microneedles of desired shape and geometry.

Moreover, the technique may be adaptable to other acrylated polymers and copolymers as well as other photo-crosslinkable polymers which can be photo-cured in the presence of free radicals. Other materials such as gelatin methacrylate (GelMA), which has been the focus of recent research pertaining to hydrogels, and is fabricated via ultraviolet crosslinking, may also be potentially used to fabricate degradable microneedles (24). However, the physical properties may need to be optimized to obtain microneedle structures strong enough to successfully penetrate the skin.

Apart from solid microneedle fabrication, the process may also be made adaptable to fabrication of hollow microneedles with adaptations needed to the photomask to create hollow microneedle structures. However, since photolithographic patterning of polymers is dependent upon ultraviolet irradiation, precise control of photomask geometry is required.

Our approach to fabrication involved first optimizing fabrication conditions to form sharp microneedles. Lens geometry, UV light intensity and spacer thickness were considered as factors influencing microneedle fabrication and geometry.

Characteristics of the thin lens in the photomask determine the degree of refraction of the UV light rays at the convex surface. The Lens makers' equation, which is used to approximate the focal length of a thin lens, was evaluated for its suitability as a predictive model for microneedle length in our fabrication process. Microneedle length measured was at least three times more than the calculated focal length regardless of UV light intensity. This indicates that the Lens makers' equation may not be an accurate predictive model in this case. This could be due to the presence of the flattened convex surface of the microlens. The irregular convex surface could have caused spherical aberration of light rays causing the path of light rays to be significantly different from that of a conventional convex thin lens (25). This aberration was seen consistently across all

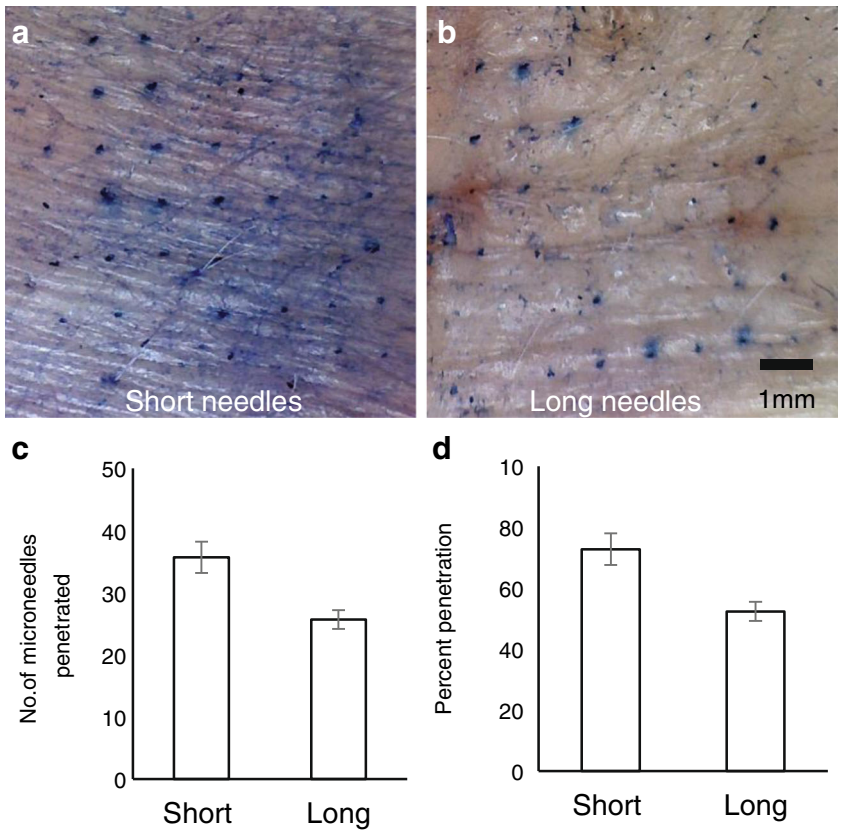


**Fig. 5** Penetration of microneedles in cadaver human skin. (**a**–**b**) Images of penetration by short and long microneedles. Respectively with the force of a thumb. (**c**) Number of successfully penetrated microneedles for short and long microneedles. (**d**) Percentage of penetration by short and long microneedles.

photomasks used. Spherical aberration allows parallel light rays that pass through the central region of the lens to focus farther away than light rays that pass through the edges of the lens leading to differential microneedle lengths. However, it was found that the lack of a perfectly curved lens did not hinder the formation of sharp-tipped microneedles after optimization of other parameters.

The intensity of UV light used for the polymerization process is another important factor with respect to the microneedle geometric properties. In this approach, an intensity of 6.44 W/cm$^2$ allowed microneedles to reach a high vertical length, with minimal structural deformation, and a desirable sharp tip diameter. Although sharper microstructures without any observable deformation were obtained at lower intensities as well, the microneedles may not possess sufficient strength and a higher intensity leads to formation of more rigid microneedles which improve the penetration efficacy.

Another phenomenon observed was that the length of microneedles increased significantly with the microneedles acquiring a more cylindrical shape, compared to the hypothesized conical shape, as intensity increased. The optical nature of light may rationalize this occurrence. Due to the flat top surface of the microlens, some light rays travel beyond the focal point in a collimated manner (26). In addition, converged light rays may also extrapolate beyond the focal point. These particular optical movements of light rays could have led to the formation of the more cylindrical portions of the needle. However, as degree of polymerization has a limit and based on the inverse-square law of light, UV light loses energy as the distance away from the source of light increases (27). This explains the tapered appearance of the microneedles observed beyond the focal point. As intensity was increased, more photons were transmitted to a further distance leading to greater uneven polymerization.

The formation of the backing layer is important to strengthen the array as a whole and to ensure reusability of the photomask. Emphasizing the importance of the backing layer, effect of the thickness of the backing layer on the strength of the microneedle shafts and extent of penetration was studied. In both different lengths of microneedle shafts, a significant fraction of the microneedles was intact after a force of more than 60 N was applied. Although fracture force for both lengths of microneedles fabricated did not vary significantly, the stronger nature of shorter microneedles was exhibited by its significantly higher penetration in human skin as evidenced from Fig. 5.

The ability for the polymeric microneedles to bend causes the actual compressive stress at the tip of the microneedle to be much lesser than the total compressive force applied by the thumb. It has been reported that to avoid sudden failure of a microneedle by buckling, and to insert the microneedle into the skin successfully, a 12:1 aspect ratio of length-to-equivalent

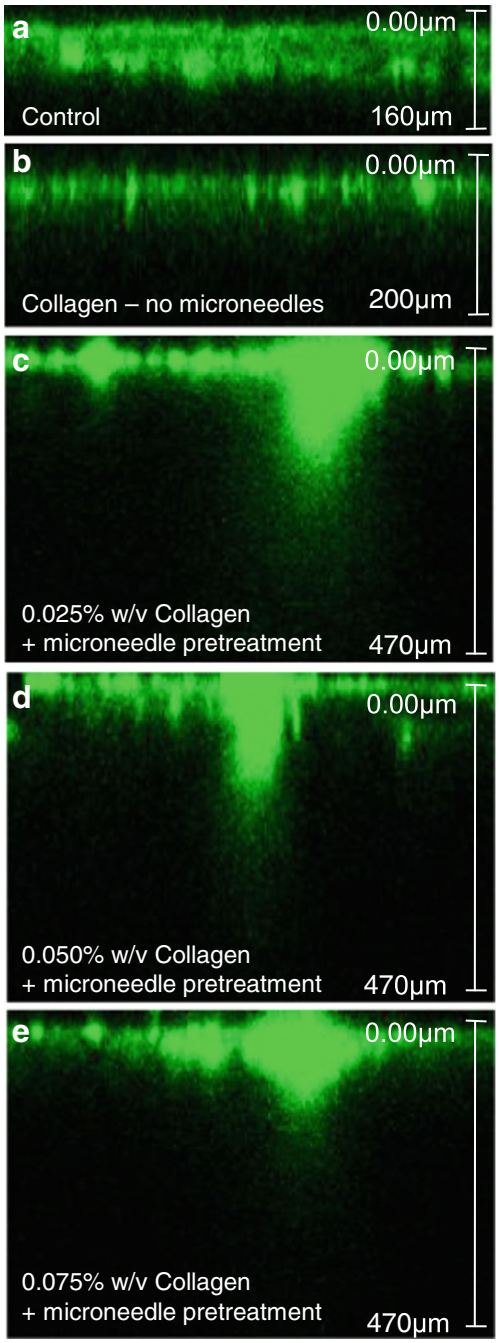


**Fig. 6** Collagen permeation in rat skin. (**a**) Auto-fluorescence of cadaver rat skin. (**b**) Fluorescence of bovine collagen type I, FITC conjugate together with auto-fluorescence of control rat skin without microneedle treatment. (**c**–**e**) Fluorescence of bovine collagen type I, FITC conjugate together with auto-fluorescence of rat skin for collagen concentrations 0.025, 0.05 and 0.075% w/v respectively.

diameter or lesser was recommended (28). In this approach, we observed that microneedles had an aspect ratio lower than 12:1. The shaft with the longest microneedle length (1,336 μm) obtained the aspect ratio of 11:1, while the shorter microneedle shaft obtained an aspect ratio of 8:1. While we observed some microneedle bending when applied on human skin, shorter microneedles with aspect ratio 8:1 penetrate better, suggesting that microneedle tip diameter is a more critical determinant of microneedle penetration. In addition, we recently found that microneedle penetration through skin was also dependent on penetration force per needle (29).

PEG based hydrogels have been used previously in numerous pharmaceutical and biomedical applications and is approved for human use (10). In an earlier study, we had extensively screened the *in vitro* toxicity of PEGDA and HMP based microneedles on various cell lines, including skin and embryonic cells and observed high cell viabilities even upon exposure for 72 h (16). The approach is amenable to other photocrosslinkable polymers, as many PEG based polymers can be easily acrylated using covalent bonding. The use of polymeric microneedles also provide an economical alternative to plastic or metallic microneedles, for e.g., commercially available microneedle array from 3 M™ cost approximately around 1 USD per array. The microneedles fabricated in this study were evaluated to cost only 0.15 USD approximately. Moreover, these polymeric microneedles can be suitably modified for a range of applications, both in drug delivery and bio-sensing.

As a model for microneedle mediated enhancement of permeation of macromolecules, we used bovine skin collagen type I, FITC conjugate. Fluorescence from collagen enabled easy analysis and visualization of depth of permeation. Diffusion of collagen molecules was greatly enhanced by the treatment of skin with the fabricated microneedles. Collagen molecules were able to diffuse past the epidermis and reach the dermal layer. Although all concentrations of collagen seemed to penetrate to equal extent, qualitatively, fluorescence signal was found to be a bit weaker at higher concentration of 0.075% w/v. This could possibly be due to some gelling that might have taken place in collagen at higher concentration when applied to skin for 4 h, even after the addition of glucose. Permeation of exogenous collagen enables it to express its pharmacological function effectively which includes activating keratinocytes in the dermis layer for reepithelialisation (30). Collagen type I has been used extensively as a substrate in culture of cells and offers a good substrate for cellular growth and proliferation (31). The situation is similar to *in vivo* in human skin where collagen supports cellular growth and healing in skin.

While collagen has been extensively used as a cosmetic product to retard skin degradation in chronologically aged skin (30,32), its efficacy from topical preparations is questionable as stratum corneum is impermeable to collagen (33). With microneedle pretreatment, collagen could permeate in significantly higher amounts and to greater depths in the skin, potentially providing a gateway for its enhanced efficacy.

The fact that higher concentrations of collagen did not significantly affect the diffusion rate, may be because epidermis and dermis layer offer a significant permeability barrier to

both small molecules and macromolecules (34) thus becoming the rate limiting step upon sufficient permeabilization of the stratum corneum. This implies that higher doses of collagen may not warrant an increased pharmacological effect when delivered transdermally. We also observed that primary structural properties of collagen type I, FITC when applied to skin post microneedle application were similar to freshly prepared solution of collagen indicating stability of collagen post microneedle application and delivery into the skin (Supplementary Material). However, it should be noted that dead rat skin samples were used in this study, which may not reflect the *in vivo* conditions.

In a recently patented technology, collagen type VII was modified by recombinant production in host cells having higher expression of prolyl 4-hydroxlase resulting in collagen having more proline residues. This collagen with increased proline residues has higher *in vivo* stability and a longer half life. The said collagen was then encapsulated in polymeric microneedles made from chitosan or alginate in pre formed micromolds. These microneedles are then used to deliver collagen VII to epidermis-dermis basement membrane in patients of dystrophic epidermolysis bullosa, a genetic disease where there is lack of functional collagen VII and leads to formation of painful blisters on the skin (35). This would be a useful approach to study collagen delivery to the skin.

## CONCLUSION

We developed a simple photolithographical method to fabricate polymeric microneedles, whose geometry could be controlled by modifying the photomask parameters in a mould free manner. The microneedles were able to penetrate cadaver human skin effectively when inserted with the force of a thumb. Microneedle shafts were also able to withstand high levels of compressive force due to the increased elasticity and shock-absorbing property of the backing layer. Irrespective of the length of the microneedle shafts, this method provides the capability to produce microneedles with similar tip diameters. In addition, we proved that collagen can be delivered transdermally up to the dermis layer for its cosmetic/pharmacological effect. The approach may be useful for the transdermal delivery of proteins and other macromolecules for localized effect within the skin layers.

## ACKNOWLEDGMENTS AND DISCLOSURES

The authors would like to acknowledge the staff of SBIC-Nikon Imaging Centre (Singapore) and Dr. Adam Cliffe from Leica Microsystems for the assistance provided in imaging the microneedle samples and skin samples. This study was supported by a National Research Foundation Grant NRF2012NRF-POC001-043 and NRF University Innovation Fund through Innovation and Entrepreneurship Practicum Grant.

## REFERENCES

1. Zhou CP, Liu YL, Wang HL, Zhang PX, Zhang JL. Transdermal delivery of insulin using microneedle rollers in vivo. Int J Pharm. 2010;392:127–33.
2. Lee JW, Choi SO, Felner EI, Prausnitz MR. Dissolving microneedle patch for transdermal delivery of human growth hormone. Small. 2011;7:531–9.
3. Raphael AP, Prow TW, Crichton ML, Chen XF, Fernando GIP, Kendall MAF. Targeted, needle-free vaccinations in skin using multi layered. Densely-packed dissolving microprojection arrays. Small. 2010;6:1785–93.
4. Hirobe S, Azukizawa H, Matsuo K, Zhai Y, Quan Y-S, Kamiyama F, *et al.* Development and clinical study of a self-dissolving microneedle patch for transcutaneous immunization device. Pharm Res. 2013;30:2664–74.
5. Kim YC, Park JH, Prausnitz MR. Microneedles for drug and vaccine delivery. Adv Drug Deliv Rev. 2012;64:1547–68.
6. Park JH, Allen MG, Prausnitz MR. Polymer microneedles for controlled-release drug delivery. Pharm Res. 2006;23:1008–19.
7. Park JH, Yoon YK, Choi SO, Prausnitz MR, Allen MG. Tapered conical polymer microneedles fabricated using an integrated lens technique for transdermal drug delivery. IEEE Trans Biomed Eng. 2007;54:903–13.
8. Zhang Y, Lin CT, Yang S. Fabrication of hierarchical pillar arrays from thermoplastic and photosensitive SU-8. Small. 2010;6:768–75.
9. Arora A, Prausnitz MR, Mitragotri S. Micro-scale devices for transdermal drug delivery. Int J Pharm. 2008;364:227–36.
10. Kochhar JS, Goh WJ, Chan SY, Kang L. A simple method of microneedle array fabrication for transdermal drug delivery. Drug Dev Ind Pharm. 2013;39:299–309.
11. Tay FEH, Iliescu C, Jing J, Miao J. Defect-free wet etching through pyrex glass using Cr/Au mask. Microsyst Technol. 2006;12:935–9.
12. Iliescu C, Chen B, Miao J. On the wet etching of Pyrex glass. Sensors Actuators A Phys. 2008;143:154–61.
13. Iliescu C, Jing J, Tay FEH, Miao J, Sun T. Characterization of masking layers for deep wet etching of glass in an improved HF/HCl solution. Surf Coat Technol. 2005;198:314–8.
14. Davis SP, Landis BJ, Adams ZH, Allen MG, Prausnitz MR. Insertion of microneedles into skin: measurement and prediction of insertion force and needle fracture force. J Biomech. 2004;37:1155–63.
15. Varshney M, Khanna T, Changez M. Effects of AOT micellar systems on the transdermal permeation of glyceryl trinitrate. Colloids Surf B: Biointerfaces. 1999;13:1–11.
16. Kochhar JS, Zou S, Chan SY, Kang L. Protein encapsulation in polymeric microneedles by photolithography. Int J Nanomedicine. 2012;7:3143–54.
17. Peebles L, Norris B. Filling 'gaps' in strength data for design. Appl Ergon. 2003;34:73–88.
18. Sugiyama K, Yamamoto K, Kamata O, Katsuda N. A simple and rapid assay for collagenase activity using fluorescence-labeled substrate. Kurume Med J. 1980;27:63–9.
19. Walsh AJ, Masters DB, Jansen ED, Welch AJ, Mahadevan-Jansen A. The effect of temperature on the autofluorescence of scattering and non-scattering tissue. Lasers Surg Med. 2012;44:712–8.
20. Zipfel WR, Williams RM, Christie R, Nikitin AY, Hyman BT, Webb WW. Live tissue intrinsic emission microscopy using multiphoton-

excited native fluorescence and second harmonic generation. Proc Natl Acad Sci U S A. 2003;100:7075–80.
21. Schonenbrucher H, Adhikary R, Mukherjee P, Casey TA, Rasmussen MA, Maistrovich FD, *et al.* Fluorescence-based method, exploiting lipofuscin, for real-time detection of central nervous system tissues on bovine carcasses. J Agric Food Chem. 2008;56:6220–6.
22. Gittard SD, Ovsianikov A, Chichkov BN, Doraiswamy A, Narayan RJ. Two-photon polymerization of microneedles for transdermal drug delivery. Expert Opin Drug Deliv. 2010;7:513–33.
23. Choi CK, Kim JB, Jang EH, Youn YN, Ryu WH. Curved biodegradable microneedles for vascular drug delivery. Small. 2012;8:2483–8.
24. Nichol JW, Koshy ST, Bae H, Hwang CM, Yamanlar S, Khademhosseini A. Cell-laden microengineered gelatin methacrylate hydrogels. Biomaterials. 2010;31:5536–44.
25. Friedman GB, Sandhu HS. Longitudinal spherical aberration of a thin lens. Am J Phys. 1967;35:628.
26. Lin TW, Chen CF, Yang JJ, Liao YS. A dual-directional light-control film with a high-sag and high-asymmetrical-shape microlens array fabricated by a UV imprinting process. J Micromech Microeng. 2008;18:095029. doi:10.1088/0960-1317/18/9/095029.
27. Dunne SM, Millar BJ. Effect of distance from curing light tip to restoration surface on depth of cure of composite resin. Prim Dent Care. 2008;15:147–52.
28. Park JH, Prausnitz MR. Analysis of mechanical failure of polymer microneedles by axial force. J Korean Phys Soc. 2010;56:1223–7.
29. Kochhar JS, Quek TC, Soon WJ, Choi J, Zou S, Kang L. Effect of microneedle geometry and supporting substrate on microneedle array penetration into skin. J Pharm Sci. 2013;102:4100–8.
30. Pilcher BK, Sudbeck BD, Dumin JA, Welgus HG, Parks WC. Collagenase-1 and collagen in epidermal repair. Arch Dermatol Res. 1998;290(Suppl):S37–46.
31. Sitterley G. Collagen attachment protocols, solubility, and stability. http://www.sigmaaldrich.com/technical-documents/articles/biofiles/collagen-product-protocols.html (accessed December 2 2013).
32. Varani J, Dame MK, Rittie L, Fligiel SEG, Kang S, Fisher GJ, *et al.* Decreased collagen production in chronologically aged skin—roles of age-dependent alteration in fibroblast function and defective mechanical stimulation. Am J Pathol. 2006;168:1861–8.
33. Anonymous. The "new" collagen: potential medical uses may abound. This protein may be altered to create products for oral surgery, treating burns, and stem cell production. Health News. 2006;12:14–5.
34. Yamaguchi K, Mitsui T, Aso Y, Sugibayashi K. Structure-permeability relationship analysis of the permeation barrier properties of the stratum corneum and viable epidermis/dermis of rat skin. J Pharm Sci. 2008;97:4391–403.
35. Marinkovich M, Lane AT, Rajadas J. Production and delivery of a stable collagen. 2012, WIPO Patent WO/2012/149136.